Bio-cementation for the mitigation of surface erosion in loess slopes based on simulation experiment

Xiaohao Sun[1] · Linchang Miao[2] · Hengxing Wang[2] · Runfa Chen[3] · Linyu Wu[2]

Abstract

Purpose Microbially induced calcite precipitation (MICP) has been shown to mitigate sand erosion; however, only few studies have used it on loess soils.

Materials and methods This study used MICP to investigate the effects of this technology on the improvement of the surface erosion resistance of loess slopes. Polyvinyl acetate (PVAc) was added to the cementation solution to further increase slope stability.

Results and discussion The obtained results showed that MICP treatment resulted in an improvement of erosion resistance and treatment with 3 L/m^2 bacterial suspension of *Sporosarcina pasteuriiand* 3 L/m^2 cementation solution (0.75 M of Ca(Ac)$_2$ and 0.75 M of urea) achieved the best erosion control and the highest surface strength. However, in rainfall simulation experiment, the eroded loss weight of loess soil in MICP-treated slopes still remained large. After adding PVAc to the cementation solution, the stability of the loess slope increased significantly and resulted in less soil loss after rainfall erosion and an increase in surface strength. With 60 g/L PVAc, the surface strength of the slope decreased by about 130 kPa compared with 40 g/L PVAc because of the thinner depth of cementation. The high erosion resistance of the slope with added PVAc could be attributed to (1) the network structure of PVAc to affix the calcium carbonate precipitation and (2) the stronger resistance to tension or shear force from PVAc. These results demonstrated that MICP-PVAc treatment significantly mitigated surface erosion of loess slopes, which presents promising potential for application in the field.

Keywords Microbially induced calcite precipitation · Polyvinyl acetate · Loess slope · Surface erosion · Calcium carbonate

✉ Xiaohao Sun
  sunxiao14hao@gmail.com

  Linchang Miao
  230159539@seu.edu.cn

  Hengxing Wang
  576477264@qq.com

  Runfa Chen
  634772923@qq.com

  Linyu Wu
  1436744679@qq.com

1 Department of Civil and Environmental Engineering, The Hong Kong Polytechnic University, Hong Kong, China

2 Institute of Geotechnical Engineering, Southeast University, Nanjing, Jiangsu 210096, China

3 Beijing Urban Construction Design & Development Group Company, Beijing 210096, China

1 Introduction

Loess soil is distributed globally and deposited by wind (Smalley 1995). In China, the loess area occupies about 630,000 km^2 and the Loess Plateau is an almost continuous area of loess soils (Gao et al. 2016). Rainfall results in raindrop splash and runoff erosion, which are the main expression forms for soil erosion. Water-induced soil erosion on the Loess Plateau is mainly caused by rainfall (Zhang and Zhu 2006; Wu et al. 2016; Wang et al. 2006). The shear strength of the loess changes due to the increase of the degree of saturation (Derbyshire et al. 2000; Peng et al. 2017). Therefore, exposure to rainfall and irrigation damages loess slopes (Zhuang et al. 2017; Leng et al. 2018; Qi et al. 2018; Luo et al. 2018).

Recently, several traditional treatment methods (e.g. engineering interventions, geotextile slope protection, and chemical treatments) have been widely used in loess slope engineering to maintain the stability of soil slopes (Juang

et al. 2019). However, the engineering interventions had application limitations and cannot improve the water erosion resistance of loess slopes. With regard to the methods of geotextile slope protection and chemical treatments, the use of 'plastic' or chemicals has negative impact on the environment because of the difficulty of degradation and corrosivity, and thus requires more attention in applications (Xu et al. 2019). Except for these traditional engineering methods, ecological intervention has also been used to improve the erosion resistance of loess slopes (Xu et al. 2019). However, the irrigation water required to maintain the afforestation process will also adversely affect the stability of the loess slopes (Juang et al. 2019). Therefore, the use of an effective and environmentally friendly method is of significance for the mitigation of loess slope surface erosion.

The cementing properties of produced calcium carbonate ($CaCO_3$) precipitation made microbially induced calcite precipitation (MICP) widely studied in geological engineering over the past decade (DeJong et al. 2006; Sun et al. 2019a). With regard to slope erosion mitigation, MICP has been reported to have promising engineering potential in increasing soil resistance against water erosion (Amin et al. 2017; Wang et al. 2018; Gao et al. 2019). MICP can also effectively improve the sand erosion resistance and mitigate water induced erosion (Shanahan and Montoya 2014; Khan et al. 2015; Salifu et al. 2016; Jiang et al. 2019; Miao et al. 2019). However, few reports investigated the use of MICP to mitigate loess slope surface erosion. Therefore, MICP was used in this study for the mitigation of surface erosion in loess slopes.

Several previous field and laboratory tests have shown that water can penetrate deep into thick loess soils due to capillary effects, which results in loss of strength (Derbyshire et al. 2000; Zhuang et al. 2017; Peng et al. 2017). Therefore, different from sands, the loess soil collapse upon wetting and thus cannot be effectively treated by MICP. The treatment effect of MICP might be impaired because of the particular characteristics of loess soils. In the study of Sun et al. (2020b), polyvinyl acetate (PVAc) emulsion was added to the reaction solution to provide additional cementation effect. As a consequence, PVAc emulsion was used in this study to further stabilize the loess surface structure, so that $CaCO_3$ produced via MICP could fill the pores and cement loess particles.

In the present study, several model loess slopes were prepared, and parts of these artificial loess slopes were treated with the MICP or MICP-PVAc method. Rainfall was simulated and the characteristics of the eroded surface and the weight of lost soils were assessed to evaluate the treatment effect. In addition, MICP-treated and MICP-PVAc-treated slope models were compared to demonstrate the improvement of erosion resistance after PVAc addition.

2 Materials and methods

2.1 Bacteria and loess soils

This study used the ureolytic bacterium *Sporosarcina pasteurii* (ATCC 11,859, from the Guangdong culture collection centre of China), which has been commonly used in previous studies (Whiffin 2004; DeJong et al. 2006; Salifu et al. 2016). The culture medium contained yeast extract 20.0 g/L, polypeptone 10.0 g/L, $(NH_4)_2SO_4$ 4 g/L, NaCl 8.0 g/L, urea 20 g/L, and distilled water. The *S. pasteurii* was grown in the medium (initial pH of 7.0) at 30 °C for 48 h.

Previous research indicated that absorbance of the suspension at a wavelength of 600 nm (OD_{600}) and urease activity (mM urea hydrolysed $\cdot$ min^{-1}) were often used to represent the growth characteristic and ureolytic activity of bacteria (Whiffin 2004; Sun et al. 2020a, 2021a; Stocks-Fischer et al. 1999). The bacterial suspension used for all tests had an identical OD_{600} of 1.205 (1.1×10^8 cell/mL, 0.712 mM urea hydrolysed/min).

Loess soils were sampled from the Loess hilly area of Ningxia province in China. The particle size of loess soils used for experiment was measured using hydrometer method in accordance with standard for geotechnical testing method in China (GB/T 50123–2019), as shown in Fig. 1. The properties of the loess soil are shown in Table 1. Moreover, the loess soils contained 5% calcite ($CaCO_3$) and 1.9% dolomite ($CaMg(CO_3)_2$). The pretreated loess soils contained calcite; however, the calcite content was similar for all samples. Therefore, the reason for the mitigation of surface erosion was contributed to the $CaCO_3$ produced via MICP.
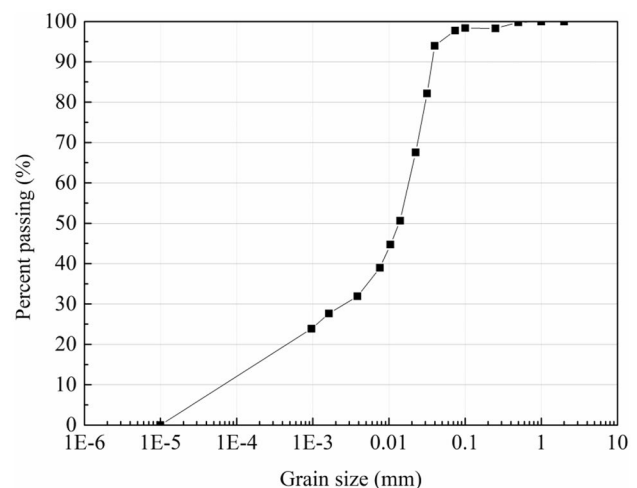

Fig. 1 Particle size distribution of loess materials

Table 1 Physical properties of the loess soils

Specific gravity	Plastic limit (%)	Liquid limit (%)	Plasticity index	Particle size composition (%)		
				Sand content (0.075–2 mm)	Silty content (0.002–0.075 mm)	Clay content (< 0.002 mm)
2.698	21.48	31.34	9.86	3.5	67.3	29.2

2.2 MICP treatment

The tests to determine loess slope erosion and the application of treatment solutions were all conducted in a cuboidal container ($0.18m \times 0.24m \times 0.04m$). The loess soil was sedimented using pluviation method to obtain the identical dry density of 1.52 g/cm^3. Three groups of loess slopes were prepared due to different volumes of the mixed solution (equal volume of bacterial suspension and cementation solution). For the subsequent application and promotion of practical engineering, the amount of the utilized mixed solution of bacterial suspension and cementation solution (0.75 M of Ca(Ac)$_2$ and 0.75 M of urea) was expressed as the spraying amount per unit area; therefore, the amounts of the mixed solution for RM-2, RM-4, and RM-6 were 2 L/m^2, 4 L/m^2, and 6 L/m^2, respectively. The test arrangements are shown in Table 2. With regard to the control sample in each group (RC-2, RC-4, and RC-6), the same amount of cementation solution was sprayed instead to comparatively observe the erosion behaviour (without bio-cementation). The mixed solution was uniformly sprayed on the artificial loess slope surfaces. Several researchers used CaCl$_2$ for application of MICP (Mahawish et al. 2018; Sun et al. 2019b). CaCO$_3$ produced from CaCl$_2$ is mainly calcite, but aragonite might be produced in the presence of calcium acetate, the bonding effect of which is better than that of calcite due to the larger specific surface area (Tittelboom et al. 2010). Calcium acetate was used to increase the bonding effect. After treatment, model slopes were air dried at 25 °C for 6 days (in experiment room) (Fig. S1 in Supporting Information).

2.3 MICP and PVAc treatment

2.3.1 Effect of PVAc addition on bacterial urease activity and CaCO$_3$ production rates

PVAc (CAS: 9003–20-7) emulsion was added to the cementation solution for better slope erosion mitigation. The PVAc addition might affect the bacterial activity or the MICP process. Consequently, before the rainfall simulation tests, the effect of the addition of PVAc on bacterial activity and the production rates of CaCO$_3$ (the ratio of the actual produced amount of CaCO$_3$ to the theoretically calculated total amount) were investigated. The amounts of PVAc were 20 g/L, 40 g/L, and 60 g/L. According to the calculation

method proposed by Whiffin (2004), the enzyme activity of the bacterial suspension was obtained after addition of PVAc. The total volume of the solution was 60 mL; and thus, the amounts of PVAc were 1.2 g, 2.4 g, and 3.6 g.

Table 2 Sample arrangements for the rainfall simulation test and surface strength test

Sample no	Treatment	Total amount of solution (L/m^2)	Test
RM-2	MICP	2	Rainfall simulation test
RC-2	CS	2	
RM-4	MICP	4	
RC-4	CS	4	
RM-6	MICP	6	
RC-6	CS	6	
RP-60	60 g/L PVAc	6	
RMP-20	MICP-20 g/L PVAc	6	
RMP-40	MICP-40 g/L PVAc	6	
RMP-60	MICP-60 g/L PVAc	6	
SM-2	MICP	2	Surface strength test
SC-2	CS	2	
SM-4	MICP	4	
SC-4	CS	4	
SM-6	MICP	6	
SC-6	CS	6	
SP-60	60 g/L PVAc	6	
SMP-20	MICP-20 g/L PVAc	6	
SMP-40	MICP-40 g/L PVAc	6	
SMP-60	MICP-60 g/L PVAc	6	

CS cementation solution, *MICP* microbially induced calcite precipitation, *PVAc* polyvinyl acetate

The slopes RM-2, RM-4, and RM-6 were treated with MICP, while the slopes RC-2, RC-4, and RC-6 were only treated with cementation solution. The slope RP-60 was treated with 60 g/L PVAc. The slopes RMP-20, RMP-40, and RMP-60 were treated with MICP, and various amounts of PVAc (20 g/L, 40 g/L, and 60 g/L) were added. The slopes SM-2, SM-4, and SM-6 were treated with MICP, while the slopes SC-2, SC-4, and SC-6 were only treated with cementation solution. The slope SP-60 was treated with 60 g/L PVAc. The slopes SMP-20, SMP-40, and SMP-60 were treated with MICP, and various amounts of PVAc (20 g/L, 40 g/L, and 60 g/L) were added

To investigate the effect of PVAc addition on the production rates of CaCO₃, PVAc was added to the cementation solution. Samples were divided into four groups according to the amount of PVAc used (0 g/L, 20 g/L, 40 g/L, and 60 g/L). Every group consisted of three parallel samples, all with an original pH of 7.0. In this study, the precipitated $CaCO_3$ was directly evaluated in transparent polypropylene tubes at a room temperature of 25 °C. Twenty millilitres of bacterial suspension of *S. pasteurii* with an OD_{600} of 1.205 was mixed with 20 mL of cementation solution. The precipitation rate of $CaCO_3$ was obtained using the acid leaching method after 48 h (Sun et al. 2018). The actual amount of precipitation was the difference between dried mass of the samples before and after rinsing with 1 M diluted hydrochloric acid. The theoretical total mass of $CaCO_3$ was evaluated by $C \times V \times M \times t$, where C represents the concentration of calcium ions in the cementation solution in mol/L, V represents the solution volume in L, M represents the molar mass of $CaCO_3$ (100.087 g/mol), and t represents the solidifying time in days.

2.3.2 Treating slope with MICP and PVAc

To compare the curing effect of PVAc addition on loess slopes, various amounts of PVAc were added to the cementation solution. Five samples were prepared, as shown in Table 2. The sample RMP-20, RMP-40, and RMP-60 were treated with MICP, and various amounts of PVAc (20 g/L, 40 g/L, and 60 g/L) were added. Sample RP-60 was sprayed the same amount of solution of PVAc (60 g/L) instead. Similarly, the slopes were dried at 25 °C for 6 days (in experiment room).

2.4 Rainfall simulation test

In reference to the method of Jiang et al. (2019), the slope angle was fixed at 30°. The rainfall intensity was controlled by a valve, at 3 mm/min (180 mm/h) to simulate a heavy storm (Fig. 2). During rainfall simulation, the water (pH of about 7.8) was sprayed uniformly by a sprayer head with 16 holes (diameter of 1 mm) on the loess slope surface. Pictures were taken by a digital camera to observe the surface erosion pattern. The dry weight of the lost loess soils collected with a collection vessel beneath the loess slope was measured at 1, 2, 3, 5, 7, 10, 15, 20, 30, 40, and 50 min. During treatment, the sealed container prevented any leakage confined the cementing solution into the pores of the treated soil for longer times. This would enhance the cementing efficiency compare to the same treatment performed into the field. This effect could be considered an upper limit for the efficiency of the treatment. New slopes were prepared and the rainfall simulation test was repeated three times to ensure the correctness of the results.

2.5 Surface strength test

Several samples were prepared with the same treatment conditions. These samples had not experienced rainfall erosion test, but surface strength test (Table 2) with a soil penetrometer (type: WISO-750–1, Juchuang company, China). After choosing six measuring points, the penetrometer (diameter of 0.5 cm) was perpendicularly pushed on 'virgin' soil surface and at time of reading the tip was 2 cm embedded into the soil. Previous researchers used surface strength to evaluate the surface treatment effect of sand soils (Ulusay and Erguler 2012; Miao et al. 2019). For loess soils, the

Fig. 2 Set-up of the rainfall simulation test

correlation between needle penetration resistance (NPR) and unconfined compressive strength (UCS) was different from sand soils. However, the surface strength in 'kPa' was still used in this study for convenient comparison.

2.6 Scanning electron microscope test

After rainfall simulation test, the surface soils in slopes SM-6 and SMP-60 were sampled for scanning electron microscope (SEM) test using the apparatus (type: JSM-6300, JEOL company, Japan) to study the crystal shape. The thickness of the soil for this test was 1–2 mm.

3 Test results and analysis

3.1 Slopes treated only with MICP

3.1.1 Rainfall erosion observation

The results from the rainfall erosion observation under simulated rainfall at 5, 10, and 20 min are shown in Fig. 3. For untreated slopes (RC-2, RC-4, and RC-6), the surface erosion pattern was similar and surface erosion could be clearly observed at 5 min. A great amount of loess soils at the top

of the slope was washed into the collection vessel (Fig. 3a). At 10 min, more loess soils were washed out from slopes (Fig. 3b); and only a small amount of loess soils remained in the container at 20 min, (Fig. 3c).

For the MICP-treaded samples, the stability of the slope was greater and no loess collapse was observed. In contrast to untreated slopes, soil at the bottom of the slope (RM-2) was washed out at 5 min (Fig. 3d) might due to surface erosion, not slope collapse. Figure 3e shows that at 10 min, the amount of soil loss was still small, but damage began to spread from the bottom. After 20 min, the slope remained significantly damaged (Fig. 3f). The damage of RM-4 was smaller and had better integrity at 5 min and 10 min (Fig. 3g and h). At 20 min, there was still a whole part on the upper of RM-4, as shown in Fig. 3i. Slope RM-6 achieved better erosion mitigation. Figure 3j shows that a portion of the slope surface at the bottom of the slope was washed away within 5 min. However, after that, less loess soil was washed out from the bottom of the slope. This was because no lower drainage was present and a large amount of the mixed solution remained at the bottom of the slope because of gravity, which cemented the loess particles together and moved the erosion position to the upper part of the sample (Fig. 3k). At 20 min, soil loss was much less significant than in the other two MICP cases (Fig. 3l).
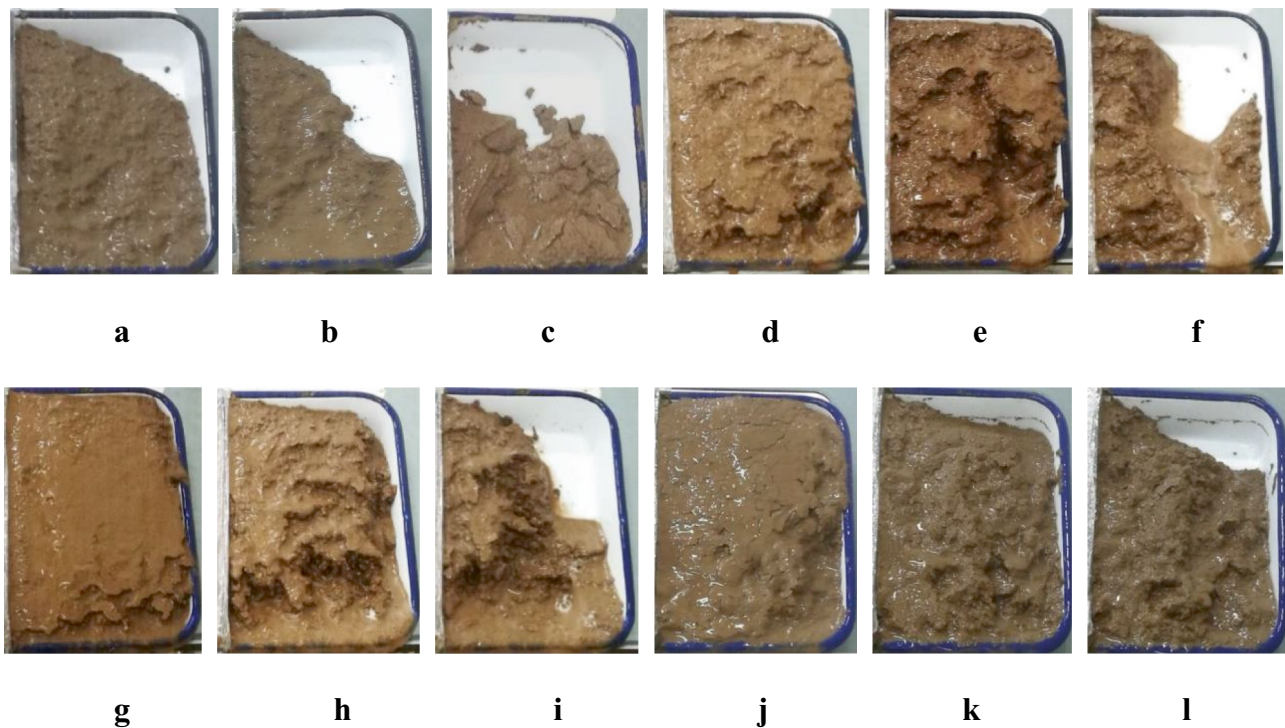

Fig. 3 Visual observation of surface erosion patterns of slopes treated with MICP and subjected to artificial rainfall for indicated durations: **a** RC-2, 5 min; **b** RC-2, 10 min; **c** RC-2, 20 min; **d** RM-2, 5 min; **e** RM-2, 10 min; **f** RM-2, 20 min; **g** RM-4, 5 min; **h** RM-4, 10 min; **i** RM-4, 20 min; **j** RM-6, 5 min; **k** RM-6, 10 min; and **l** RM-6, 20 min. Note: The slopes RM-2, RM-4, and RM-6 were treated with MICP, while the slope RC-2 was only treated with cementation solution

3.1.2 Soil loss weight and surface strength

For untreated slopes, spraying more cementation solution would not mitigate surface erosion (Fig. 4). After erosion for 50 min, the value even reached 90%. When the amount of solution was 4 L/m^2 or 6 L/m^2, the MICP treatment resulted in a highly significant decrease of the percentage of eroded soil compared with the samples sprayed cementation solution ($P < 0.01$). The rate of the percentage of accumulative soil loss weight decreased at first. Sample RM-2 and RM-4 seemed reactivating higher erosion rates between 30 and 50 min. The total percentages of eroded loess soils in RM-2, RM-4, and RM-6 after 50 min of exposure to rainfall were about 80%, 65%, and 47%, respectively. The same reactivating phenomenon happened for RM-6 at 40 to 50 min; however, the total percentage of eroded soil highly significantly decreased with the amount of solution increasing from 4 to 6 L/m^2 ($P < 0.01$). The cementation effect was worse than that reported by Jiang et al. (2019). The reason was that the total volume of the bacterial solution and the cementation solution used was less and the curing time was shorter. The results were consistent within the rainfall simulation tests. A better cementation effect was contributed to a higher mass of CaCO$_3$.

Figure 5 shows that in response to spraying cementation solution from 2 to 4 L/m^2, the surface strength increased significantly from 156 to 260 kPa ($P < 0.05$). This was because the loess sample contained a portion of clay soil, which would shrink and thus increase strength. However, with spraying cementation solution 6 L/m^2, the surface strength insignificantly increased to 327 kPa ($P > 0.05$). In addition, the salt would provide the cementation effect and also increase the strength of loess soil in dry conditions. After treatment with MICP, the surface strength further increased because of the produced CaCO$_3$. For the amount of solution of 4 L/m^2, the increase was significant ($P < 0.05$); and for the amount of solution of 6 L/m^2, the increase was highly significant ($P < 0.01$). With increased concentration of PVAc, the surface strength always significantly increased ($P < 0.05$). The loess slope RM-6 had a clearly larger surface strength (442 kPa), which resulted from more CaCO$_3$ precipitation. This result confirmed that CaCO$_3$ precipitation can also cement loess particles.

In conclusion, MICP treatment indeed improves loess slope stability, mitigate surface erosion, and increases surface strength. The soil loss in RM-6, however, was still significantly higher than the results of previous research in sand (Salifu et al. 2016; Jiang et al. 2019). Therefore, PVAc addition was proposed to effectively and efficiently control loess slope surface erosion.

3.2 Slopes treated with MICP and PVAc

3.2.1 Effect of PVAc addition on bacterial urease activity and CaCO$_3$ production rates

To investigate the effect of PVAc addition on bacterial urease activity, various concentrations of PVAc were added to urea solution. After adding PVAc, the urease activity only experienced a slight fluctuation, as shown in Fig. 6a. The treatment effect was affected by the amount of CaCO$_3$ produced. It was necessary to study the effect of PVAc addition

Fig. 4 Accumulative soil loss weight of slopes treated with MICP. Note: MICP is microbially induced calcite precipitation. The slopes RM-2, RM-4, and RM-6 were treated with MICP, while the slopes RC-2, RC-4, and RC-6 were only treated with cementation solution
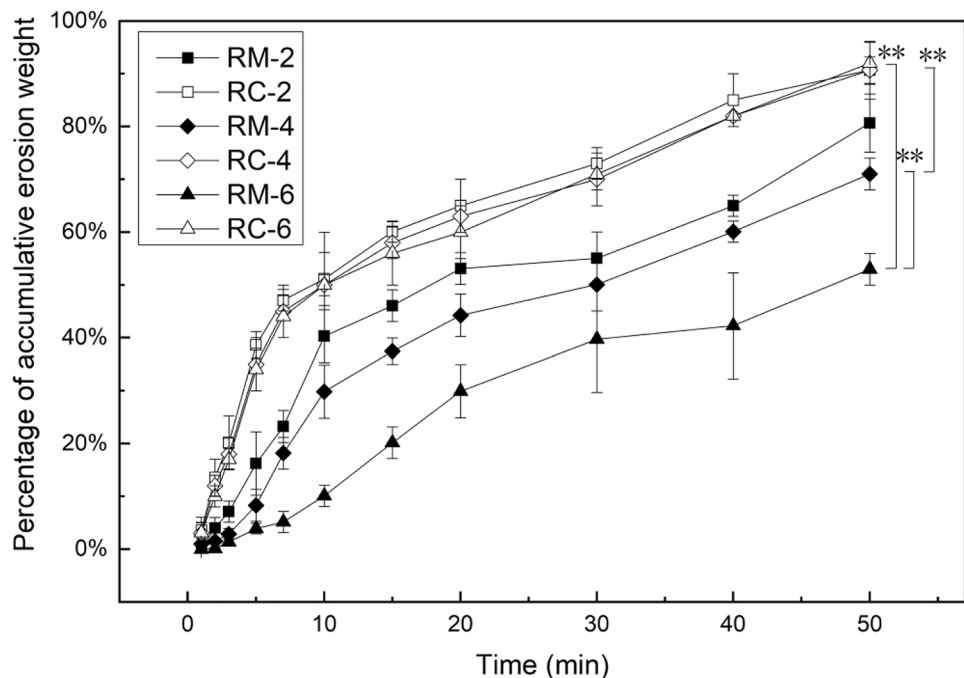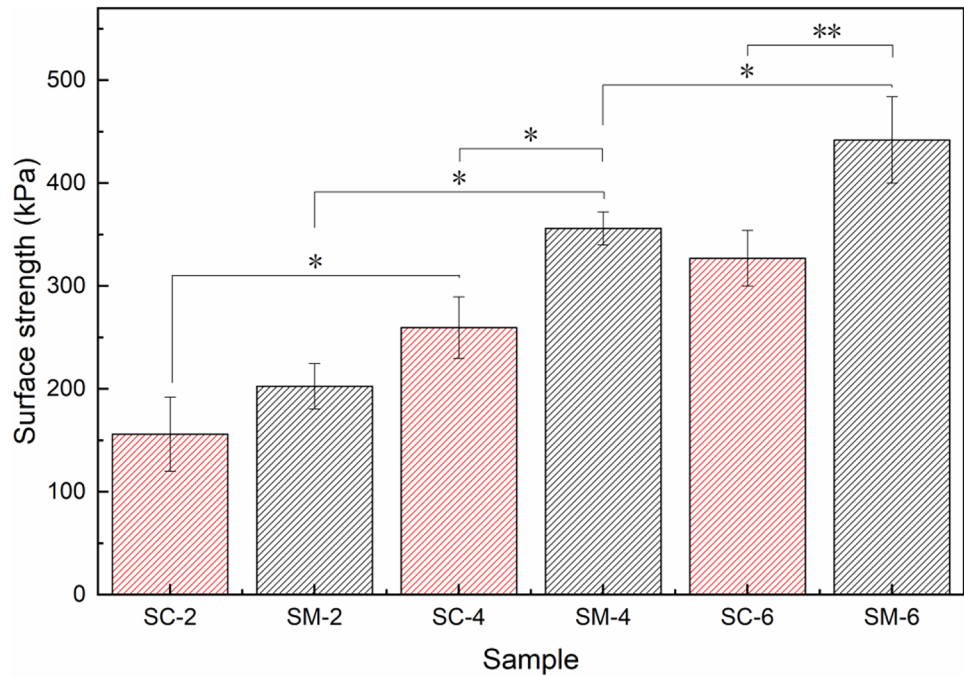
Fig. 5 Comparison of surface strength of slopes treated with bio-cementation and without bio-cementation


on the production rates of $CaCO_3$. Figure 6b shows that with increasing PVAc concentration, there was little change on production rates for $CaCO_3$. There is no significant difference between the values in Fig. 6a and b ($P < 0.05$). Therefore, adding PVAc had little impact on both the urease activity and production rates for $CaCO_3$.

3.2.2 Rainfall erosion observation

After combined treatment with MICP and PVAc, the stability of the loess slope improved significantly. Because

changes could not be observed within a short time, the time span of observation in Fig. 7 increased compared that use for Fig. 3.

In contrast to slopes treated with MICP alone, no slope collapse or soil surface erosion was observed at 10 min (Fig. 7a, d, and g). For RMP-20, a crack at the upper slope emerged at 20 min (Fig. 7b). At 50 min, the slope was destroyed because water entered from the interior of the sample through cracks and destroyed the internal structure (Fig. 7c). Observing the samples after destruction showed that there was a thin hard surface crust. This hard surface
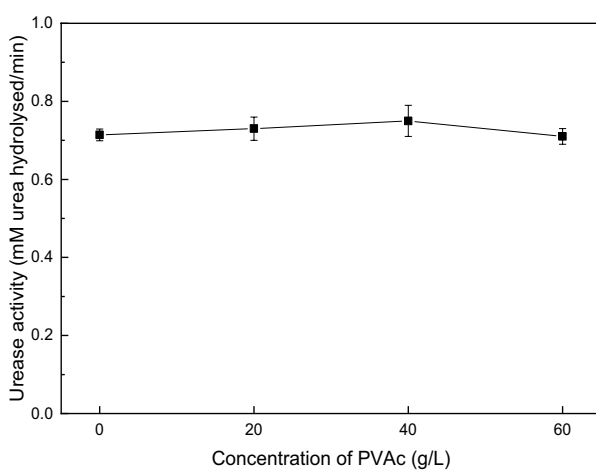
a
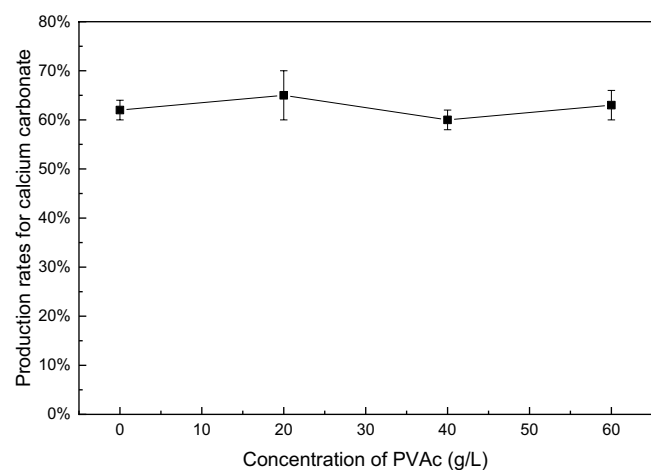
b

Fig. 6 Urease activity and production rates of calcium carbonate after PVAc addition: **a** urease activity; **b** production rates for calcium carbonate. Note: PVAc is polyvinyl acetate
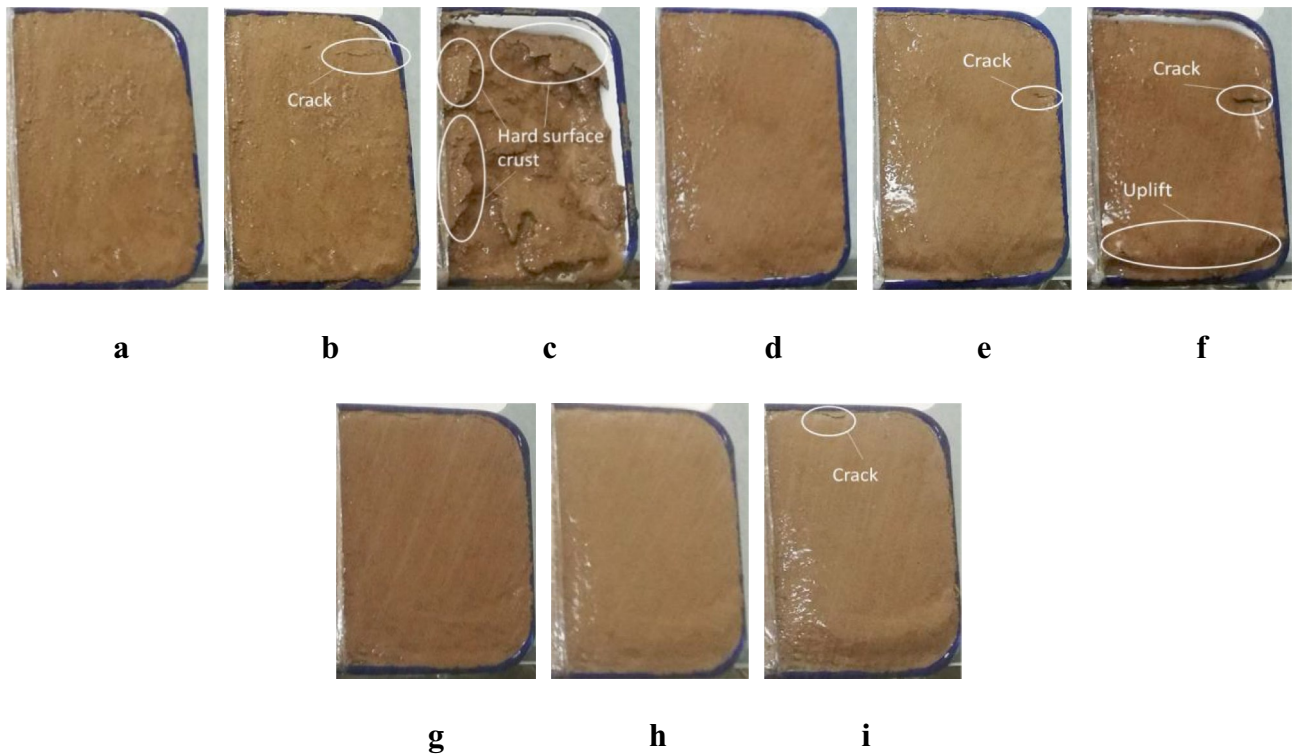
Fig. 7 Visual observation of surface erosion patterns of slopes treated with MICP and PVAc: **a** RMP-20, 10 min; **b** RMP-20, 20 min; **c** RMP-20, 50 min; **d** RMP-40, 10 min; **e** RMP-40, 20 min; **f** RMP-40, 50 min; **g** RMP-60, 10 min; **h** RMP-60, 20 min; **i** RMP-60, 50 min.

Note: MICP is microbially induced calcite precipitation. PVAc is polyvinyl acetate. The slopes RMP-20, RMP-40, and RMP-60 were treated with MICP, and various amounts of PVAc (20 g/L, 40 g/L, and 60 g/L) were added

crust was primarily composed of $CaCO_3$ minerals (Jiang et al. 2019). With regard to slope RMP-40, Fig. 7e shows a smaller crack at 20 min. However, the growth speed of this crack was lower and after 50 min of exposure to rainfall, the crack still remained small due to better cementing effect. The uplift happened at the bottom of the slope and it did not break after 50 min (Fig. 7f). This was because water entered the interior of the sample (RMP-40), causing part of the loess soil to flow down. The slope RMP-60 had a more resistant and homogeneous surface compared with the other two slopes. Figure 7h shows that no crack appeared within 20 min. However, a small crack appeared on the upper part of the specimen, at 50 min; and this uplift was much smaller than that of slope RMP-40 (Fig. 7i).

3.2.3 Soil loss weight and surface strength

The slope RP-60 experienced a large loess soils loss from 30 to 50 min (Fig. 8), which was attributed to a lower cementation limit. With regard to slopes treated with both MICP and PVAc, the weights of the lost loess soils were much lower than those for RP-60 and RM-6. There were highly significant decreases between RP-60 and RMP-60,

RM-6 and RMP-20 ($P < 0.01$). During the initial 15 min, the amounts of lost loess soils were almost zero. After that, a small amount of soil in slope RMP-20 was washed out; however, the accumulative loess soils loss weights of slopes RMP-40 and RMP-60 still remained zero because of their better cementing effect. The eventual accumulative loess loss weights of RMP-40 and RMP-60 after 50 min of exposure to rainfall were only 3.04 and 0 g, respectively. The better curing effect of RMP-40 and RMP-60 was contributed to the higher concentration of PVAc, which highly significantly decreased the eventual accumulative loess loss weights ($P < 0.01$) compared with RMP-20.

The surface strengths of slope SP-60 and SM-6 were smaller than the slopes treated with both MICP and PVAc (Fig. 9). When the concentration of PVAc was 20 g/L, there is no significant increase of surface strength between SMP-20 and SP-60, or SMP-20 and SM-6 ($P > 0.05$). However, with PVAc concentration increasing to 40 g/L, there was a highly significant increase in surface strength for the loess slope SMP-40 (657 kPa) ($P < 0.01$). However, with adding PVAc of 60 g/L, the surface strength of slope SMP-60 highly significantly decreased more than that of slope SMP-40 ($P < 0.01$), while still remaining higher than that of

Fig. 8 Accumulative soil loss weight of slopes treated with MICP and PVAc. Note: MICP is microbially induced calcite precipitation. PVAc is polyvinyl acetate. The slope RP-60 was treated with 60 g/L PVAc. The slope RM-6 was treated with MICP alone, and slopes RMP-20, RMP-40, and RMP-60 were treated with MICP, and various amounts of PVAc (20 g/L, 40 g/L, and 60 g/L) were added
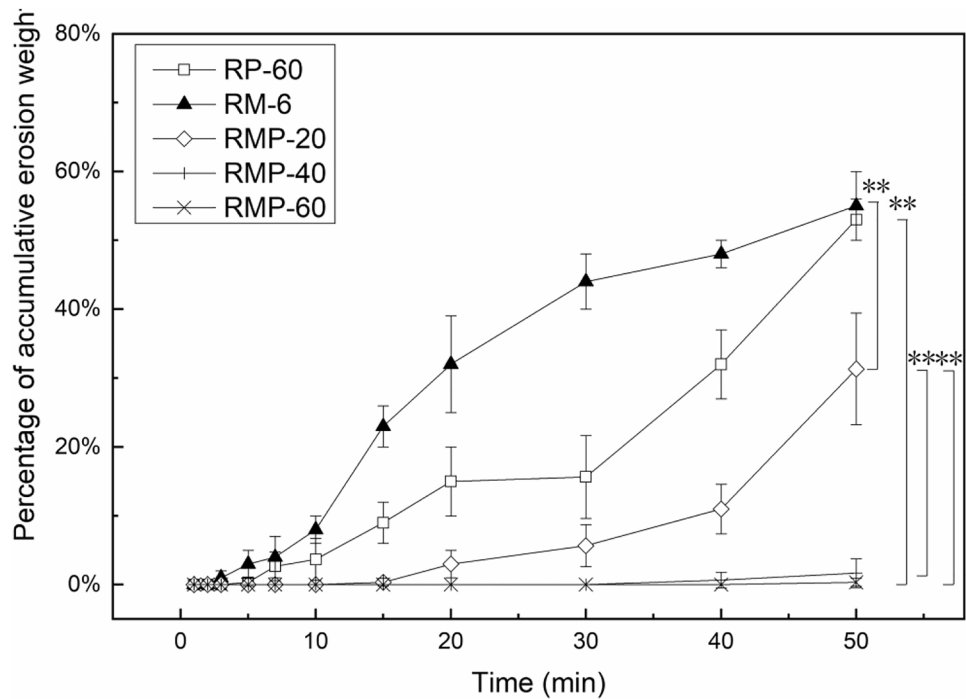
slope SMP-20 and no significant difference between SMP-60 and SMP-20 ($P > 0.05$). This suggests that the thickness of cementation of SMP-60 was smaller, while the depths of measuring points for surface strengths were all about 0.02 m, resulting in lower surface strength. The reason is further analysed in the "Thickness of cemented layer" section.

3.2.4 Thickness of cemented layer

After the rainfall simulation test, the samples were oven dried at 75 °C for 48 h. Treated soils were sampled perpendicular to the slope surface and the thicknesses of the cemented layer were obtained via calliper (Table 3). For

Fig. 9 Surface strength of slopes treated with MICP and PVAc as reported in Table 2. Note: MICP is microbially induced calcite precipitation. PVAc is polyvinyl acetate
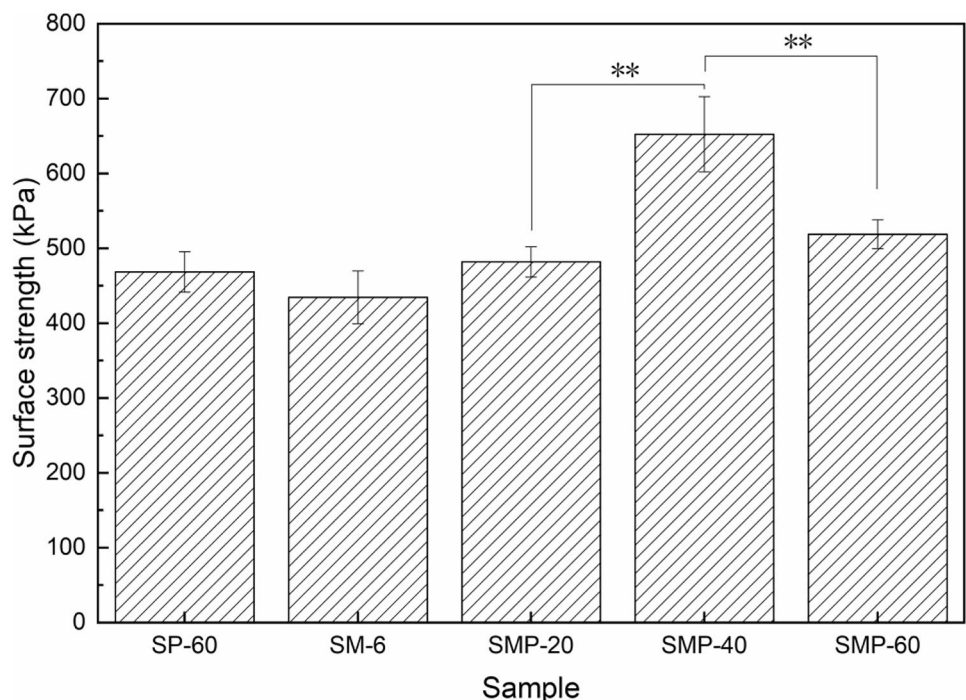
Table 3 Cementation layer thickness of slopes treated with different methods

Sample no	Average cemented layer thickness (mm)	Viscosity (mPa·s)	Treatment
SP-60	10.1	370	60 g/L PVAc
SM-6	24.0	/	MICP
SMP-20	17.4	149	MICP-20 g/L PVAc
SMP-40	10.6	256	MICP-40 g/L PVAc
SMP-60	9.3	370	MICP-60 g/L PVAc

MICP microbially induced calcite precipitation, *PVAc* polyvinyl acetate
Viscosity refers to the viscosity of PVAc solution

SM-6 treated with MICP, the thickness of the cemented layer was 24.0 mm. For SMP-20, SMP-40, and SMP-60, the thicknesses of the cemented layer were much lower than in SM-6. The viscosity of the PVAc emulsion limited the imbibition depth of the soil when treated with PVAc, eventually leading to smaller thicknesses of the cemented layer than slope SP-60 (10.1 mm). With regard to SMP-60, despite the thinner cemented layer, MICP-PVAc treatment allowed for a higher strength against surface erosion than PVAc treatment alone and MICP treatment alone. It was found that a higher concentration of PVAc in cementation solution resulted in a thinner cemented layer. This was because PVAc addition would clog near-surface soil pores. With higher PVAc concentration, the mixed solution would be harder to percolate into deeper soil. Furthermore, even if the cemented layer thicknesses of SMP-40 and SMP-60 were less than those of SM-6 and SMP-20, their erosion resistance was significantly better (Figs. 7 and 8). The high erosion resistances of SMP-40 and SMP-60 were attributed to (1) the network structure of PVAc to affix the CaCO$_3$ precipitation and (2) the stronger cementation effect from MICP and PVAc. Both hypotheses will be further analysed in the "Discussion" section.

3.2.5 Scanning electron microscope test

SEM testing can be used to compare the difference among soil specimen from a microscopic perspective (Delage et al. 2006). Figure 10a shows that in response to MICP treatment, a large number of CaCO$_3$ crystals were produced between loess particles. In addition to their bridge function, CaCO$_3$ crystals were also deposited on the surface of loess particles as schematized in Fig. 11. Compared to SM-6, the MICP-PVAc treatment on SMP-60 coated several loess particles by PVAc and CaCO$_3$ crystals together, which formed a layer-like film. Moreover, loess particles were contacted by PVAc and CaCO$_3$ crystals together (Fig. 10b).

Furthermore, in response to MICP treatment, most CaCO$_3$ crystals were vaterite with a size of about 3–5 μm (Fig. 10c). In addition to spherical crystals, few amorphous crystals were found. However, in contrast to SM-6, most CaCO$_3$ crystals in Fig. 10d were amorphous crystals. The size of CaCO$_3$ crystals remained below 1 μm, and these small crystals were clumped together.

4 Discussion

4.1 Treatment of MICP for loess slope surface erosion mitigation

Rainfall-erosion resistance depends on cementation microstructure, shearing mode, confining stress, and relative densities (among other factors) (Dejong et al. 2006; Chang et al. 2015; Zhan et al. 2016; Sun et al. 2021c). In the application of MICP method for sandy-slope surface erosion control, with a concentration of reagent below 1.0 M, CaCO$_3$ crystals preferably stay between particle contacts (Seagren and Aydilek 2010; Jiang et al. 2019). In other words, most particle contacts are bridged by CaCO$_3$ crystals, which lead to stronger intergranular binding. The CaCO$_3$ crystals between particle contacts allowed for an effective improvement of the shear resistance of treated soils (Nafisi et al. 2020a, 2020b). The predominant particle contacts deposition is also the major contributor to erosion resistance (Salifu et al. 2016). Previous studies have proved that the MICP method has promising engineering potential to mitigate the sandy-slope surface erosion (Amin et al. 2017; Gao et al. 2019; Wang et al. 2018; Shanahan and Montoya 2014; Khan et al. 2015; Salifu et al. 2016).

Similarly, in the loess slope surface erosion mitigation, the intergranular binding also contributes to the enhanced erosion resistance. Several previous studies proved that CaCO$_3$ crystals between particle contacts are more effective than coated ones in terms of enhancing intergranular binding (DeJong et al. 2010; Al Qabany et al. 2012; Al Qabany and Soga 2013). Therefore, the cementation solution should be in favour of new CaCO$_3$ crystal nucleation than existing crystal growth. In this study, the loess soil used was much smaller than sands. When the concentration of reagents in the cementation solution was higher, most of the formed CaCO$_3$ would stack up on the top of surface soil instead of producing between granular cementation. Moreover, with lower concentration of reagent, there would be predominantly unclogged large voids. Therefore, the concentration of reagent in the cementation solution was 0.75 M for the loess slope surface erosion mitigation. With regard to the MICP-treated loess slope SM-6, a large number of CaCO$_3$ crystals were produced between loess particles (Fig. 10a), which was the reason for the enhanced erosion resistance. The concentration of reagent in this study was lower than that for the sand-slope S2 in Jiang et al. (2019); therefore, the size of CaCO$_3$ crystals in loess slope SM-6 in this study was smaller.
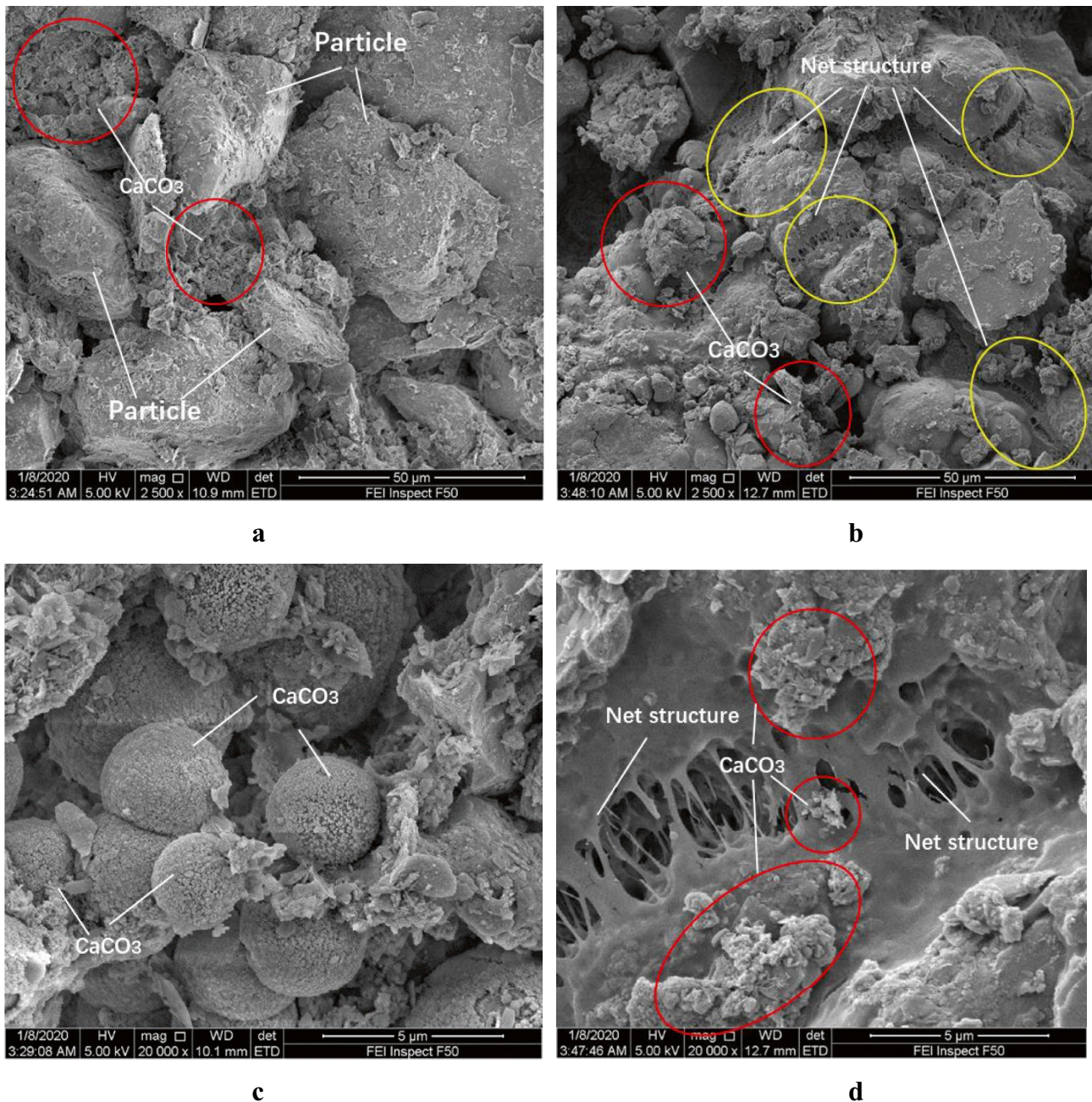
Fig. 10 SEM images of treated slopes after rainfall simulation tests: **a** SM-6, magnification=2500×; **b** SMP-60, magnification=2500×; **c** SM-6, magnification=20,000×; **d** SMP-60, magnification=20,000×.

Note: The slope SM-6 was treated with MICP alone, and the slope SMP-60 was treated with MICP, and 60 g/L of PVAc

In treated loess, the MICP treatment also created bridges between loess particles. However, in contrast to sand-slopes, there are a large number of large pores in loess slopes (Sun et al. 2021b). After solidification, these large pores could not be completely filled by CaCO₃ precipitation. Consequently, the whole skeleton of loess soil could not be well stabilized with the MICP method alone. When the MICP-treated loess

slopes experienced a prolonged rainfall erosion, water can penetrate deep into thick loess soils, which results in loss of strength (Derbyshire et al. 2000; Zhuang et al. 2017; Peng et al. 2017). Therefore, the enhanced erosion resistance resulted from the MICP method was not sufficient and a better treatment was necessary to mitigate loess slope surface erosion.
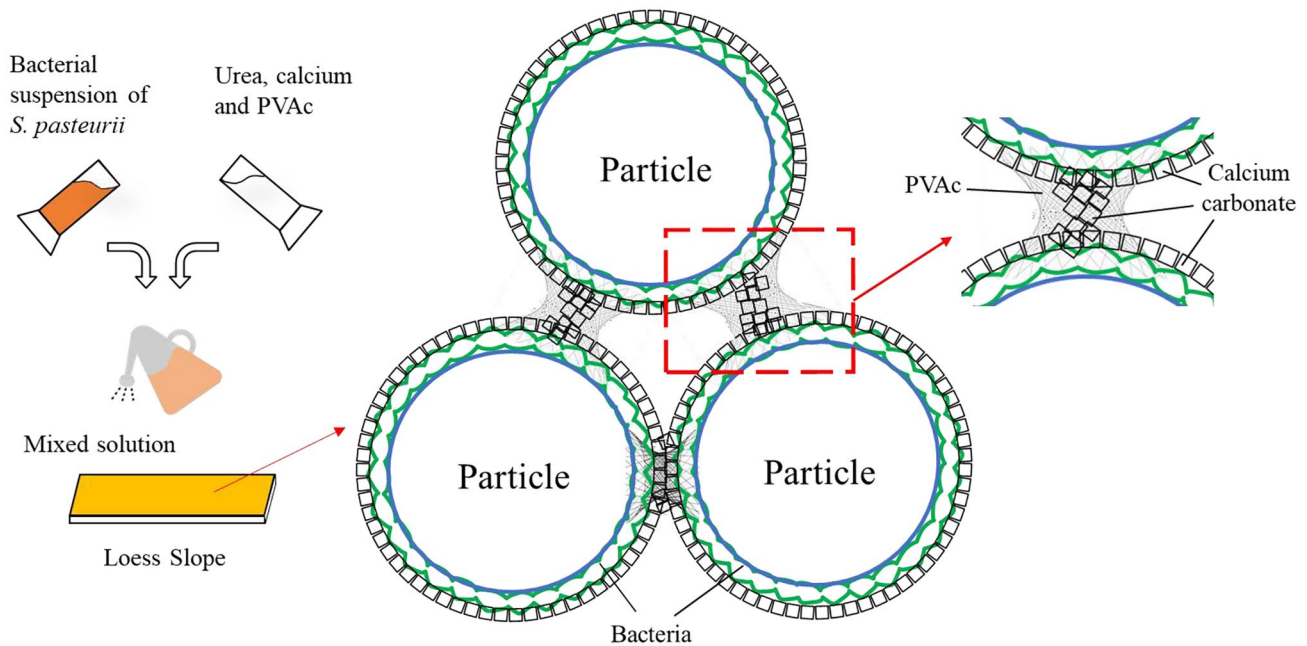
Fig. 11 Schematic diagram of cementation between particles

4.2 Treatment of MICP and PVAc together

PVAc was added in this study for better slope erosion mitigation. The PVAc emulsion is mainly composed of a vinyl acetate (VAc) monomer (Dossi et al. 2010; Rosdi and Ariffin 2016; Ahmed et al. 2017; Gordon et al. 2019). Several non-traditional additives such as polymers, geo-polymers, and biopolymers have been studied for soil strength improvement (Bu et al. 2019; Ghasemzadeh and Modiri 2020; Soldo et al. 2020). In previous studies, these additives (e.g. acrylic polymers, PVAc, and Persian gum) have been proved to be nontoxic and can be categorized as environmentally friendly water-based soil stabilizers (Zhang et al. 2018; Bu et al. 2019; Ghasemzadeh et al. 2020). Therefore, the PVAc emulsion used herein does not negatively impact the environment.

If PVAc was used for slope treatment, the volume would be large, resulting in higher costs. PVAc emulsions have satisfactory gap-filling properties (Shields 1984). Therefore, similarly to Sun et al. (2020b), PVAc and MICP was used together to bond particles and form a more stable structure (Fig. 11). With low PVAc concentration, the microstructure forms a network structure (Jazi et al. 2019). This decreases the cost by decreasing the required PVAc concentration.

In addition, the network structure of PVAc might have four advantages in the improvement of loess slope surface erosion resistance:

The first advantage is that the network structure of PVAc can provide bonding force and tension force between loess particles (Fig. 10b), which is beneficial to stabilize the macroporous skeleton of loess and enhance the surface erosion resistance. The better stability of MICP-PVAc-treated loess slopes has been demonstrated by Figs. 8 and 9.

The second advantage is that the network structure of PVAc is beneficial to affix the $CaCO_3$. Miao et al. (2019) also reported that polyacrylamide had the same effect. Most $CaCO_3$ crystals in SMP-60 were held in place by PVAc (Fig. 10d). The $CaCO_3$ crystals were small and clumped together. The reason was that the mineral structure of $CaCO_3$ crystals was affected by PVAc, so that the crystals could not grow into a large sphere, but rather, grew into a group of amorphous crystals. The more stable spatial net structure in SMP-60 was confirmed by SEM photo. Zhao et al. (2016) also demonstrated that poly (acrylic acid) (PAA) can work with enzyme-induced carbonate precipitation (EICP) to form more stable spatial structure.

De Jong et al. (2006) found that for samples treated with MICP, most of the failure interface was inside $CaCO_3$, i.e. the generated $CaCO_3$ was fractured inside after failure. Therefore, it was necessary to increase the shear resistance. Sun et al. (2021c) reported that the addition of PVAc increased friction angle and cohesion of treated soils. With the addition of PVAc, the network structure can provide stronger shear resistance, thus avoiding $CaCO_3$ fracture inside and improving the slope stability. It is the third advantage of the PVAc addition.

With regard to the fourth advantage, compared with the loess slope SM-6 (MICP treatment alone), in SMP-60 with MICP-PVAc treatment, PVAc and $CaCO_3$ crystals resembled a film to coat loess particles (Fig. 10b). The film can prevent water from penetrating deep into thick loess soils, i.e. the film

can prevent rainfall from damaging loess skeleton structure. The film might further mitigate the rainfall erosion, which also deserves further proof and study.

The combination of these two additives in soil improvement was investigated for the first time. However, the tests conducted in this paper have demonstrated that the MICP treatment can improve the erosion resistance of loess slopes and the addition of PVAc can further improve the slope stability. More macro or microscale tests can be conducted in subsequent studies to prove its effectiveness for practical applications.

5 Ecological compatibility

Ecological intervention is still a good method to improve the erosion resistance of loess slopes despite its limitations (Xu et al. 2019). If the MICP-PVAc method proposed in this study was combined with the ecological intervention, the stability of loess slope surface would be significantly improved. Firstly, the loess particles would be cemented by $CaCO_3$ crystals and PVAc, providing more time for plant growth and impairing the effect of irrigation water. Secondly, the voids of loess soils were filled, and a crust layer formed, which allowed for an improvement of water retention capacity (Chang et al. 2015; Zhan et al. 2016; Saffari et al. 2019). Better water retention capacity enabled the quick plant growth (Tran et al. 2019). Moreover, in this study, both the nutrient medium used for bacterial culture and urea in the cementation solution contained carbon and nitrogen fertilizer for plant growth. The ecological compatibility of EICP has been preliminary studied by Sun et al. (2020b). They found grass seeds could survive in the alkaline environment produced by the EICP; and the area with the combined EICP-PVAc and grass seeds treatment had a higher surface strength. Therefore, the MICP-PVAc method proposed in this study had good ecological compatibility. However, the thickness of crust layer also affected the seedlings' bud rate (Zhan et al. 2016); therefore, with regard to the ecological compatibility of combined EICP-PVAc and grass seeds treatment, it deserves further study.

6 Mitigation of landslides

The landslide of loess slopes is related to internal factors (e.g. slope structure, topography, and physical and chemical properties of soil) and external factors (e.g. rainfall, human engineering activities). The shallow landslides are often induced by surface water erosion and groundwater erosion (Van Asch et al. 1999; Huo et al. 2019). Rainfall is the most important factor to trigger landslides (Huo et al. 2020). Water flow is formed due to the confluence process, which promotes the development of surface erosion. The water flow caused several channels, which had a strong downcutting effect on the structure of loess slopes, leading to the damage of loess slopes. With the further development of downcutting effect, collapses or landslides often happen because of gravity. The eroded loess soil along with the water flow is also an important effect to trigger landslides. It is unlikely that a mountain side is entirely treated by MICP-PVAc to prevent erosion; however, the MICP-PVAc treatment is effective to mitigate the surface water erosion. For the treated loess slopes, water flow can hardly form channels; therefore, the downcutting effect is too weaker to damage the structure of loess slopes. In addition, the layer-like film formed by PVAc can avoid the increase in runoff and erosion in the lower areas of the slope. In conclusion, the MICP-PVAc treatment is also beneficial to mitigate landslides.

For the traditional treatment methods (e.g. engineering interventions, geotextile slope protection, and chemical treatments) used to maintain the stability of soil slopes, the engineering interventions had application limitations and cannot improve the water erosion resistance of loess slopes. The geotextile slope protection and chemical treatments have negative impact on the environment (Xu et al. 2019). Ecological intervention is beneficial to control land degradation and mitigate erosion, but the irrigation water adversely affects the stability of the loess slopes. The MICP-PVAc method proposed is environmentally friendly and can quickly and effectively mitigate surface erosion, which has significant application potential for the mitigation of surface erosion in loess slopes.

7 Conclusions

Bio-cementation tests were conducted to investigate the effects of the MICP technology on the improvement of loess slope surface erosion resistance. MICP treatment improved erosion resistance, especially the treatment with 6 L/m² of mixed solution (total percentage of eroded loess soils of 47% and the highest surface strength of 442 kPa). The soil loss, however, is still large. Therefore, PVAc addition was proposed to further improve slope stability. Addition of PVAc had little impact on urease activity and production rates for $CaCO_3$. The eventual accumulative loess loss weights of RMP-40 and RMP-60 after 50 min of exposure to rainfall were only 3.04 and 0 g, respectively. The surface strength of loess slope SMP-40 even reached 657 kPa. The high erosion resistance for EICP-PVAc treatment was attributed to (1) the network structure of PVAc to affix the $CaCO_3$ precipitation and (2) the stronger resistance to tension or shear force from PVAc. The method proposed is effective and efficient for loess slope erosion control, with promising potential for application in the field thanks to the limited concentration of PVAc needed (~40 g/L) cost ~2USD/Kg.

Declarations

References

Ahmed M, Abd-Elhamid M, Sarhan A, Hassan A (2017) Characteristic and thermal stimulated depolarization current of poly (vinyl chloride-co-vinyl acetate-co-2-hydroxy propyl acrylate) Znonanocomposite. Glob J Phys 5:585–594

Al Qabany A, Soga K (2013) Effect of chemical treatment used in MICP on engineering properties of cemented soils. Géotechnique 63(4):331–339

Al Qabany A, Soga K, Santamarina C (2012) Factors affecting efficiency of microbially induced calcite precipitation. J Geotech Geoenviron Eng 138(8):992–1001

Amin M, Zomorodian S, Kelly B (2017) Reducing the hydraulic erosion of sand using microbial-induced carbonate precipitation. Proc Inst Civ Eng Ground Improv 170(2):112–122

Bu F, Liu J, Bai Y, Prasanna Kanungo D, Song Z, Kong F, Pan C (2019) Effects of the preparation conditions and reinforcement mechanism of polyvinyl acetate soil stabilizer. Polymers 11(3):506

Chang I, Prasidhi A, Im J, Shin H, Cho G (2015) Soil treatment using microbial biopolymers for anti-desertification purposes. Geoderma 253–254:39–47

DeJong J, Fritzges M, Nüsslein K (2006) Microbially induced cementation to control sand response to undrained shear. J Geotech Geoenviron Eng 132(11):1381–1392

DeJong J, Mortensen B, Martinez B, Nelson D (2010) Bio-mediated soil improvement. Ecol Eng 36(2):197–210

Delage P, Marcial D, Cui Y, Ruiz X (2006) Ageing effects in a compacted bentonite: a microstructure approach. Géotechnique 56(5):291–304

Derbyshire E, Meng XM, Dijkstra T (2000) Landslides in the thick loess terrain of North-West China. John Wiley and Sons Ltd, London

Dossi M, Liang K, Hutchinson R, Moscatelli D (2010) Investigation of free-radical copolymerization propagation kinetics of vinyl acetate and methyl methacrylate. J Phys Chem B 114:4213–4222

Gao H, Li Z, Jia L, Li P, Xu G, Ren Z, Pang G (2016) Capacity of soil loss control in the loess plateau based on soil erosion control degree. J Geogr Sci 26(4):457–472

Gao Y, Tang X, Chu J, He J (2019) Microbially induced calcite precipitation for seepage control in sandy soil. Geomicrobiol J 36(4):366–375

Ghasemzadeh H, Mehrpajouh A, Pishvaei M, Mirzababaei M (2020) Effects of curing method and glass transition temperature on the unconfined compressive strength of acrylic liquid polymer–stabilized kaolinite. J Mater Civ Eng 32(8):04020212

Ghasemzadeh H, Modiri F (2020) Application of novel Persian gum hydrocolloid in soil stabilization. Carbohyd Polym 246:116639

Gordon P, Bierwagen J, Preston M (2019) Stevens Ferdinand Rodriguez George B. Kauffman Alan N. Gent. Major industrial polymers. Encyclopædia Britannica, inc.

Huo A, Wang X, Liang Y, Jiang C, Zheng X (2019) Integrated numerical model for irrigated area water resources management. J Water Clim Change, jwc2019042

Huo A, Yang L, Peng J, Cheng Y, Jiang C (2020) Spatial characteristics of the rainfall induced landslides in the Chinese Loess Plateau. Hum Ecol Risk Assess Int J 2020:1–16

Jazi M, SA A, Haddadi S, Ghaderi S, Azamian F (2019) *In situ* emulsion polymerization and characterization of PVAc nanocomposites including colloidal silica nanoparticles for wood specimens bonding. J Appl Polym Science

Jiang N, Tang C, Yin L, Xie Y, Shi B (2019) Applicability of microbial calcification method for sandy-slope surface erosion control. J Mater Civ Eng 31(11):04019250

Juang C, Dijkstra T, Wasowski J, Meng X (2019) Loess geohazards research in China: advances and challenges for mega engineering projects. Eng Geol 251:1–10

Khan M, Amarakoon G, Shimazaki S, Kawasaki S (2015) Coral sand solidification test based on microbially induced carbonate precipitation using ureolytic bacteria. Mater Trans 56(10):1725–1732

Leng Y, Peng J, Wang Q, Meng Z, Huang W (2018) A fluidized landslide occurred in the Loess Plateau: a study on loess landslide in South Jingyang Tableland. Eng Geol 236:129–136

Luo H, Wu FQ, Chang JY, Xu JB (2018) Microstructural constraints on geotechnical properties of Malan Loess: a case study from Zhaojiaan landslide in Shaanxi province. China Eng Geol 236:60–69

Mahawish A, Bouazza A, Gates W (2018) Effect of particle size distribution on the bio-cementation of coarse aggregates. Acta Geotech 13(4):1019–1025

Miao L, Wu L, Sun X, Li X, Zhang J (2019) Method of solidifying desert sands with enzyme-catalysed mineralization. Land Degrad Develop

Nafisi A, Mocelin D, Montoya B, Underwood S (2020a) Tensile strength of sands treated with microbially induced carbonate precipitation. Can Geotech J 57(10):1611–1616

Nafisi A, Montoya B, Evans T (2020b) Shear strength envelopes of biocemented sands with varying particle size and cementation level. Journal of Geotechnical and Geoenvironmental Engineering 146(3):04020002

Peng J, Wang G, Wang Q, Zhang F (2017) Shear wave velocity imaging of landslide debris deposited on an erodible bed and possible movement mechanism for a loess landslide in Jingyang, Xi'an, China. Landslides 14:1503–1512

Qi X, Xu Q, Liu F (2018) Analysis of retrogressive loess flow slides in Heifangtai. China Eng Geol 236:119–128

Rosdi M, Ariffin A (2016) Evaluation of flow ability response in EVA emulsion preparation with different vinyl acetate percentage by intrinsic viscosity measurement. Procedia Chem 19:455–461

Saffari R, Nikooee E, Habibagahi G, Van Genuchten M (2019) Effects of biological stabilization on the water retention properties of unsaturated soils. J Geotech Geoenviron Eng 145(7), 04019028.1–04019028.12

Salifu E, MacLachlan E, Iyer K, Knapp C, Tarantino A (2016) Application of microbially induced calcite precipitation in erosion mitigation and stabilisation of sandy soil foreshore slopes: a preliminary investigation. Eng Geol 201: 96–105

Seagren E, Aydilek A (2010) Biomediated geomechanical processes. In Environmental biology, 319–349. Hoboken, NJ: Wiley

Shanahan C, Montoya B (2014) Strengthening coastal sand dunes using microbial-induced calcite precipitation. In Proc. GeoCongress 2014, GSP 234, edited by M. Abu-Farsakh, X. Yu, and L. R. Hoyos. Reston, VA: ASCE

Shields J (1984) Adhesives handbook, 3rd edn. Butterworths Heinemann, London

Smalley I (1995) Making the material: the formation of silt sized primary mineral particles for loess deposits. Quat Sci Rev 14(7–8):645–651

Soldo A, Miletić M, Auad M (2020) Biopolymers as a sustainable solution for the enhancement of soil mechanical properties. Sci Rep 10(1):1–13

Stocks-Fischer S, Galinat JK, Bang SS (1999) Microbiological precipitation of $CaCO_3$. Soil Biol Biochem 31(11):1563–1571

Sun X, Miao L, Tong T, Wang C (2018) Improvement of microbial-induced calcium carbonate precipitation technology for sand solidification. J Mater Civ Eng 30(11):04018301

Sun X, Miao L, Tong T, Wang C (2019a) Study of the effect of temperature on microbially induced carbonate precipitation. Acta Geotech 14(3):627–638

Sun X, Miao L, Wu L, Chen R (2019b) Improvement of bio-cementation at low temperature based on Bacillus megaterium. Appl Microbiol Biotechnol 103(17):7191–7202

Sun X, Miao L, Chen R (2020a) The application of bio-cementation for improvement in collapsibility of loess. Internatl J Environ Sci Technol (5)

Sun X, Miao L, Yuan J, Wang H, Wu L (2020b) Application of enzymatic calcification for dust control and rainfall erosion resistance improvement. Sci Total Environ 143468.

Sun X, Miao L, Wu L, Wang H (2021a) Theoretical quantification for cracks repair based on microbially induced carbonate precipitation (micp) method. Cement Concrete Compos (1):103950

Sun X, Miao L, Wang H, Chen R, Guo X (2021b) Improvement of characteristics and freeze-thaw durability of solidified loess based on microbially induced carbonate precipitation. Bull Eng Geol Environ

Sun X, Miao L, Wang H, Yuan J, Fan G (2021c) Enhanced rainfall erosion durability of enzymatically induced carbonate precipitation for dust control. Sci Total Environ 148369

Tittelboom K, Belie N, Muynck W (2010) Use of bacteria to repair cracks in concrete. Cem Concr Res 40(1):157–166

Tran A, Chang I, Cho G (2019) Soil water retention and vegetation survivability improvement using microbial biopolymers in drylands. Geomech Eng 17(5):475–483

Ulusay R, Erguler Z (2012) Needle penetration test: evaluation of its performance and possible uses in predicting strength of weak and soft rocks. Eng Geol 149:47–56

Van Asch T, Buma J, Van Beek L (1999) A view on some hydrological triggering systems in landslides. Geomorphology 30:25–32

Wang H, Wang Q, Shao M (2006) Laboratory experiments of soil nutrient transfer in the loess slope with surface runoff during simulated rainfall. Trans Chin Soc Agric Eng 22(6):39–44

Wang X, Tao J, Bao R, Tran T, Tucker-Kulesza S (2018) Surficial soil stabilization against water-induced erosion using polymermodified microbially induced carbonate precipitation. J Mater Civ Eng 30(10):04018267

Whiffin V (2004) Microbial CaCO3 precipitation for the production of biocement. Murdoch University, Perth, Australia

Wu L, Liu X, Ma X (2016) Spatiotemporal distribution of rainfall erosivity in the Yanhe River watershed of hilly and gully region. Chinese Loess Plateau Environ Earth Sci 75(4):315

Xu R, Li X, Yang W, Jiang C, Rabiei M (2019) Use of local plants for ecological restoration and slope stability: a possible application in Yan'an, Loess Plateau, China. Geomat Nat Haz Risk 10(1):2106–2128

Zhan Q, Qian C, Yi H (2016) Microbial-induced mineralization and cementation of fugitive dust and engineering application. Constr Build Mater 121:437–444

Zhang Y, Pang B, Yang S, Fang W, Yang S, Yuan T, Sun R (2018) Improvement in wood bonding strength of poly (vinyl acetate-butyl acrylate) emulsion by controlling the amount of redox initiator. Materials 11(1):89

Zhang Y, Zhu Q (2006) Analysis on eroded rainfall characteristics of Loess Plateau. Res Environ Arid Land 06:99–103

Zhao Z, Hamdan N, Shen L, Nan H, Almajed A, Kavazanjian E, He X (2016) Biomimetic hydrogel composites for soil stabilization and contaminant mitigation. Environ Sci Technol 50(22):12401–12410

Zhuang J, Peng J, Wang G, Iqbal J, Wang Y, Li W, Xu Q, Zhu X (2017) Prediction of rainfall-induced shallow landslides in the Loess Plateau, Yan'an, China, using the TRIGRS model. Earth Surf Process Landf 42(6):915–927